



## Long-term satellite observations show continuous increase of vegetation growth enhancement in urban environment

Peng, Xi; Jiang, Shucheng; Liu, Shuguang; Valbuena, Ruben; Smith, Andy; Zhan, Yang; Shi, Yi; Ning, Ying; Feng, Shuailong; Gao, Haiqiang; Wang, Zhao

### Science of the Total Environment

DOI:

[10.1016/j.scitotenv.2023.165515](https://doi.org/10.1016/j.scitotenv.2023.165515)

Published: 10/11/2023

Peer reviewed version

[Cyswllt i'r cyhoeddiad / Link to publication](#)

*Dyfyniad o'r fersiwn a gyhoeddwyd / Citation for published version (APA):*

Peng, X., Jiang, S., Liu, S., Valbuena, R., Smith, A., Zhan, Y., Shi, Y., Ning, Y., Feng, S., Gao, H., & Wang, Z. (2023). Long-term satellite observations show continuous increase of vegetation growth enhancement in urban environment. *Science of the Total Environment*, 898, Article 165515. <https://doi.org/10.1016/j.scitotenv.2023.165515>

#### Hawliau Cyffredinol / General rights

Copyright and moral rights for the publications made accessible in the public portal are retained by the authors and/or other copyright owners and it is a condition of accessing publications that users recognise and abide by the legal requirements associated with these rights.

- Users may download and print one copy of any publication from the public portal for the purpose of private study or research.
- You may not further distribute the material or use it for any profit-making activity or commercial gain
- You may freely distribute the URL identifying the publication in the public portal ?

#### Take down policy

If you believe that this document breaches copyright please contact us providing details, and we will remove access to the work immediately and investigate your claim.

# **Long-term satellite observations show continuous increase of vegetation growth enhancement in urban environment**

Xi Peng<sup>a#</sup>, Shucheng Jiang<sup>a#</sup>, Shuguang Liu<sup>a\*</sup>, Rubén Valbuena<sup>b</sup>, Andy Smith<sup>b</sup>, Yang Zhan<sup>a</sup>, Yi Shi<sup>a</sup>, Ying Ning<sup>a</sup>, Shuailong Feng<sup>a</sup>, Haiqiang Gao<sup>a</sup>, Zhao Wang<sup>a</sup>

<sup>a</sup> College of Life Science and Technology, and National Engineering Laboratory for Applied Technology in Forestry & Ecology in South China, Central South University of Forestry and Technology, Changsha 410004, China

<sup>b</sup> School of Natural Sciences, Bangor University, Bangor, UK

<sup>#</sup>These authors contributed equally to this work and should be considered co- first authors

<sup>\*</sup>Corresponding author at: College of Life Science and Technology, Central South University of Forestry and Technology, Changsha, China

E-mail address: [shuguang.liu@yahoo.com](mailto:shuguang.liu@yahoo.com) (S. Liu)

# Highlights

Proposed a long-term framework to quantify urbanization impacts on vegetation.

Urbanization decreased regional EVI due to direct surface-replacement impact.

Urban environment stimulated an enhancement of vegetation growth over time.

Growth enhancement offset about 28% to 44% of direct EVI loss.

## 1. Abstract

2       Urbanization shows continuous expansion and development, ushering in the co-evolution  
3 of urban environments and vegetation over time. Recent remote sensing-based studies have  
4 discovered prevalent vegetation growth enhancement in urban environments. However,  
5 whether there is a temporal evolution of the growth enhancement remains unknown and  
6 unexplored. Here we expanded the existing framework for assessing the long-term impact of  
7 urbanization on vegetation greenness (enhanced vegetation index, EVI) using long time series  
8 of remote sensing images and applied it in Changsha, the capital city of Hunan province in  
9 China. Results showed that vegetation growth experienced widespread enhancement from  
10 2000 to 2017, and increased 1.8 times from 2000 to 2017, suggesting strong continuous  
11 adaptive capability of vegetation to urban conditions. Although the overall impact of  
12 urbanization was negative due to the replacement of vegetated surfaces, the growth  
13 enhancement nevertheless offset or compensated the direct loss of vegetated cover during  
14 urbanization in the magnitude of 28% in 2000 to 44% in 2017. Our study also revealed large  
15 spatial heterogeneity in vegetation growth response among various districts at different

16 urbanization levels and found an emergent trend under the observed spatial heterogeneity  
17 toward an asymptotic maximum with urbanization, showing EVI converges to 0.22 in highly  
18 urbanized areas. We further found that the positive effect of urbanization on vegetation  
19 growth is a function of urbanization intensity and time, which implies that the effect of the  
20 urban environment on vegetation can be simulated and predicted, and can be verified in more  
21 cities in the future. Our study is the first to successfully quantify long-term spatial patterns on  
22 the co-evolution of urbanization and vegetation, providing a new understanding of the  
23 continuous adaptive responses of vegetation growth to urbanization and shedding light on

24 predicting biological responses to future environmental change.

25 Keywords: urbanization, vegetation growth, temporal evolution, regional disparity,

26 indirect effect, time-series analysis

## 27 **2. Introduction**

28 Urbanization represents the process of urban landscape transformation and urban  
29 environment intensification, with significant modification to the vegetation cover and growth,  
30 to entail both changes in urban environments and vegetated structures that co-evolve over  
31 time (Hutyra et al., 2011; Li et al., 2013; Shi et al., 2021). The changes in urban environments  
32 can be regarded as a baseline trajectory (e.g., localized warming, or increasing CO<sub>2</sub>  
33 enrichment), serving as a “harbinger” for future global change (Grimm et al., 2008). Thus, the  
34 adaptation of urban vegetation to these environmental changes can serve as a natural  
35 experiment for projected responses to future climate change (Youngsteadt et al., 2015).  
36 Remote sensing-based approaches have provided opportunities to monitor the spatial and  
37 temporal dynamics of vegetation growth in urbanization-affected environments (Jia et al.,  
38 2018; Zhao et al., 2016). However, long time-series analyses of the co-evolution of urban  
39 environments and vegetation have been rarely reported, which hinders us from further  
40 understanding and inferring about the future impact of urbanization on vegetation. Thus, it is  
41 necessary to explore the long-term vegetation responses to urbanization, to provide empirical  
42 evidence and theoretical basis to better understand the biological responses to future  
43 urbanization processes and climate change.

44 A few remote sensing-based studies have found a prevalent vegetation growth  
45 enhancement in urban environments (Jia et al., 2018; Zhang et al., 2022; Zhao et al., 2016;

46 Zhong et al., 2019). However, whether there is temporal evolution of growth enhancement  
47 remains unknown and unexplored. Most existing studies only compared differences in  
48 vegetation growth between limited years and may not capture long-term interannual changes  
49 in growth enhancement (Jia et al., 2018; Zhao et al., 2016; Zhong et al., 2019). Because the  
50 observed variations in vegetation responses may be transient and pulsating over limited  
51 periods, analysis without long-term observations might not reveal the gradual responses and  
52 adaptation of vegetation to altered environmental conditions (Tang et al., 2021). The need to  
53 quantify and understand the long-term aggregated effects of urbanization (including changing  
54 land cover, various atmospheric conditions, human management conditions, etc.) on  
55 vegetation growth has motivated us to expand the existing framework for analyzing the  
56 temporal dynamic evolution of vegetation growth in cities.

57 Accurate characterization of the urbanization impact on vegetation is complicated by  
58 significant regional differences in land cover and land use history, plant species assemblage,  
59 human behavior, and microclimate change. Previous studies usually relied on a rural-urban  
60 gradient or urbanization intensity (i.e., the percentage of developed imperviousness) to  
61 describe the regional differences (Li et al., 2020; Zhou et al., 2014). Because cities are often  
62 divided into districts and each district has its urban core and fringe areas, and the different  
63 development levels for each district also increase the regional disparity and possible  
64 vegetation consequences (de Jong et al., 2016; Liu et al., 2020). Such variability in the  
65 developmental stage exhibits more subtle spatial differences over time, leading to a more  
66 pronounced heterogeneity in vegetated cover and annual variation (Zhang et al., 2023).  
67 Therefore, analyzing the vegetation responses to urbanization at the district level would more  
68 accurately depict the process of urbanization, including development, redevelopment, and  
69 renewal of each district, and might shed new light on the response of vegetation growth to  
70 urbanization.

71 The overall goal of this study was to examine the long-term evolution of the impacts of  
72 urbanization on holistic urban vegetation greenness (quantified by enhanced vegetation index,  
73 EVI) by expanding the Zhao and colleagues' framework, which developed a general  
74 conceptual framework for quantifying the direct and indirect effects of urbanization on  
75 vegetation growth (Zhao et al., 2016). The work is applied in Changsha, the capital city of  
76 Hunan province, China with many city-subordinated districts showing obvious spatial and  
77 temporal variations in regional and urban development. Specifically, we aimed to (1) quantify  
78 temporal evolution patterns of urbanization impacts on vegetation growth; (2) investigate  
79 regional disparity of EVI trends along urbanization intensity; (3) investigate processes and  
80 temporal evolutions of EVI in rural and highly urbanized areas of all districts.

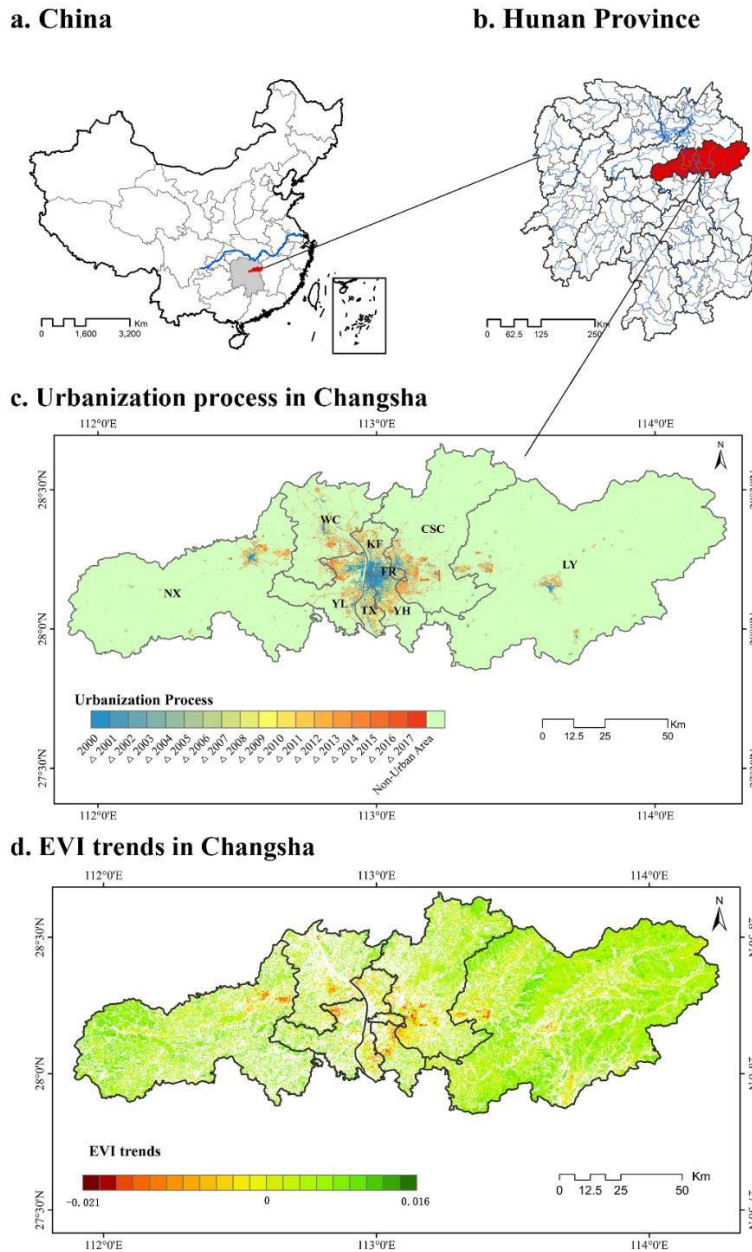
## 81 **2. Methods**

### 82 **2.1. Study Area**

83 Changsha (27°51'N to 28°41'N, 111°53'E to 114°15'E) is the capital city of Hunan  
84 province, south-central of China, with a total area of 11,819 km<sup>2</sup> (Fig. 1). It is in the hilly  
85 area in the south of the Yangtze River, and the terrain is undulating with an elevation  
86 difference of 1586.3 meters. The city is dominated by a typical subtropical monsoon  
87 climate with four distinct seasons. The annual mean temperature is about 17.2°C, and annual  
88 mean precipitation is approximately 1451.4 mm, and the annual mean rainy days are 152  
89 days, mainly in spring and summer (the climate data was provided by the China  
90 Meteorological Data Network (<http://data.cma.gov.cn/site/index.html>, accessed date: 10  
91 August 2021) and based on 1987-2015 normal). The potential vegetation in Changsha is  
92 mainly subtropical evergreen broad-leaved forest.

93            Changsha is divided into nine administrative districts, namely Furong District (FR, 43  
94   km<sup>2</sup>), Tianxin District (TX, 141 km<sup>2</sup>), Kaifu District (KF, 188 km<sup>2</sup>), Yuhua District (YH, 287  
95   km<sup>2</sup>), Yuelu District (YL, 545 km<sup>2</sup>), Wangcheng district (WC, 947 km<sup>2</sup>), Ningxiang city (NX,  
96   2,906 km<sup>2</sup>), Liuyang city (LY, 5,006 km<sup>2</sup>), and Changsha county (CSC, 1,756 km<sup>2</sup>) (Fig. 1c).  
97   The nine administrative districts show obvious variations in regional development,  
98   manifesting a coexistence of developing and highly developed regions. There was a  
99   development priority sequence among districts from 2000 to 2017 with the main urban area  
100   (the districts of FR, TX, KF, YH, and YL) first prioritized for development in the early years  
101   and then WC, NX, LY, and CSC in recent years (Fig.1c) (Liu et al., 2020).





102

103 **Fig.1** Spatial and temporal distribution of urbanization process and EVI trends from 2000 to

104 2017 in Changsha (c,d), the capital city of Hunan province (b) in China (a). (c) The dark blue

105 of “2000” represents the urban areas in 2000, the “△” means the increase of urban areas

106 compared with the previous year, and the abbreviations represent nine districts of Changsha.

107 (d) EVI trends indicate the slope of the linear regression between EVI and time (year) for

108 each pixel from 2000 to 2017, greater than 0 means that EVI was increasing with the years

109 and less than 0 means decreasing with the years.

## 110 **2.2. Time series of EVI during the growing season**

111 EVI can be used to measure vegetation performance or growth, and it shows higher  
112 performance than the Normalized Difference Vegetation Index (NDVI) in capturing  
113 vegetation conditions in impervious areas (Yu et al., 2017). The EVI product (MOD13Q1)  
114 from the MODIS satellite, with a spatial resolution of 250 m and a temporal resolution of 16  
115 days, was used in this study. To further eliminate the influence of atmospheric conditions, the  
116 maximum-value-composite (MVC) technique (Fang, 2004) was used to obtain monthly time-  
117 series EVI data. The time series of EVI in each year were calculated by averaging the monthly  
118 values of EVI in the growing season (Zhao et al., 2018).

## 119 **2.3. Calculation of the urbanization intensity**

120 The urbanization intensity ( $\beta$ ) of a MODIS pixel was defined as the percentage of  
121 impervious surfaces within the pixel, ranging from 0 (completely covered by vegetation) to 1  
122 (urban cover with no vegetation) (Zhao et al., 2016). The impervious surface data spanning  
123 2000-2017 at 30 m  $\times$  30 m resolution from the Finer Resolution Observation and Monitoring –  
124 Global Land Cover system of Tsinghua University (<http://data.ess.tsinghua.edu.cn/>, accessed  
125 date: 14th August 2020) (Chen et al., 2019; Gong et al., 2019) were used to calculate  $\beta$  of  
126 each MODIS pixel (i.e., the proportion of land cover map pixels belonging to the built-up area  
127 within the pixel).

## 128 **2.4. Analysis of EVI trends**

129 EVI trend was defined as the slope of the linear regression between EVI and time (year)  
130 for each pixel from 2000 to 2017 (Yu et al., 2017). EVI trends were determined for each pixel  
131 using Sen's slope estimator (Sen, 1968), which has the advantage of dealing well with the

132 presence of missing data and the ability to resist outliers and keep unbiased and accurate for  
133 skew and heteroscedastic data (Liu et al., 2015a). For these reasons, this robust non-  
134 parametric method has been used widely in vegetation time-series change studies (He et al.,  
135 2015). The change of the EVI trends along the urbanization intensity gradient from 0 to 1 was  
136 investigated using boxplots in Changsha and its nine administrative regions, and 50% quantile  
137 regression analyses (i.e., median regression) were used to explore the change of EVI trend  
138 along the urbanization intensity gradient.

## 139 **2.5. Quantification of the Impacts of Urbanization on EVI**

140 According to the conceptual framework defined by Zhao et al. (2016), the impact of  
141 urbanization on vegetation growth can be systematically quantified as direct impact and  
142 indirect impact (Zhao et al., 2016). The direct impact refers to the EVI reduction caused by  
143 direct area loss of vegetated surfaces during urban development, and the indirect impact is the  
144 effects imposed on vegetation by the altered urban environment (e.g., warming, increased CO<sub>2</sub>  
145 and nitrogen deposition, pollution, and improved management practices) (Jia et al., 2018;  
146 Zhao et al., 2016). Conceptually, the vegetation index of an urban pixel is composed  
147 of contributions from vegetation and non-vegetated areas, which can be expressed by the  
148 following formulae (Zhao et al., 2016):

$$149 \quad V_{obs} = (1 + \omega)(1 - \beta)V_v + \beta V_{nv} \quad (1)$$

150 where  $\beta$  is urbanization intensity,  $V_{obs}$  is the observed VI of the pixels (EVI in this study),  
151  $V_v$  is the background vegetation index not affected by urbanization (i.e.,  $\beta = 0$ ,  $VI = V_v$ ),  $\omega$  is  
152 the overall impact of urbanization produced, and  $V_{nv}$  is the VI of impervious surfaces (i.e.,  
153  $\beta = 1$ ,  $VI = V_{nv}$ ).

154 A set of quantitative measures are defined in Zhao and colleagues' framework to evaluate

155 the impacts of urbanization. The zero-impact line, the relative indirect influence, and the  
 156 growth offset rate were calculated by Zhao et al. (2016). The zero-impact line, representing  
 157 the conditions that vegetation growth was not indirectly affected by urbanization, can be  
 158 defined as follows:

$$159 \quad V_{zi} = (1 - \beta)V_v + \beta V_{nv} \quad (2)$$

160 where  $V_{zi}$  was the theoretical VI of a 250-m resolution pixel, defined by  $V_v$  ( $\beta = 0$ ,  $VI =$   
 161  $V_v$ ) and  $V_{nv}$  ( $\beta = 1$ ,  $VI = V_{nv}$ ).

162 The relative indirect influence is expressed as:

$$163 \quad \omega_\tau = \frac{V_{obs} - V_{zi}}{V_{zi}} \quad (3)$$

164 The growth offset rate ( $\tau$ ) between indirect and direct effects can be defined as:

$$165 \quad \tau = \frac{V_{obs} - V_{zi}}{V_v - V_{zi}} \quad (4)$$

166  $\tau$  represents how much the growth change of remaining vegetation caused by the indirect  
 167 impact can compensate (if  $\tau$  was positive) or exacerbate (if  $\tau$  was negative) the loss of  
 168 vegetated productive surface owing to direct built-up replacement.

169 A cubic polynomial model was used to fit the  $EVI \sim \beta$  relationship of each year:  $y = a_0 +$   
 170  $a_1x + a_2x^2 + a_3x^3$ , where  $y$  is the mean observed EVI for a given  $\beta$  (i.e.,  $x$ ). The  
 171 intercept ( $a_0$ ) was fixed to be the empirical background EVI value observed, as it depended on  
 172 the trend of EVI change and greatly reduced the influence of EVI outliers (Jia et al., 2018;  
 173 Zhao et al., 2016; Zhong et al., 2019).

174 This study determined  $V_{nv}$  ( $\beta = 1$ ,  $VI = V_{nv}$ ) by the mean EVI value of fully urbanized  
 175 pixels ( $\beta = 1$ ) in years from 2000 to 2017. To ensure that the value of  $V_{nv}$  was obtained

176 without interference from vegetation activities, we used a high-resolution Google Earth image  
177 visual inspection of  $\beta = 1$  pixel to avoid uncertainties from the imperviousness data. The  
178 resultant average  $V_{nv}$  was 0.066.

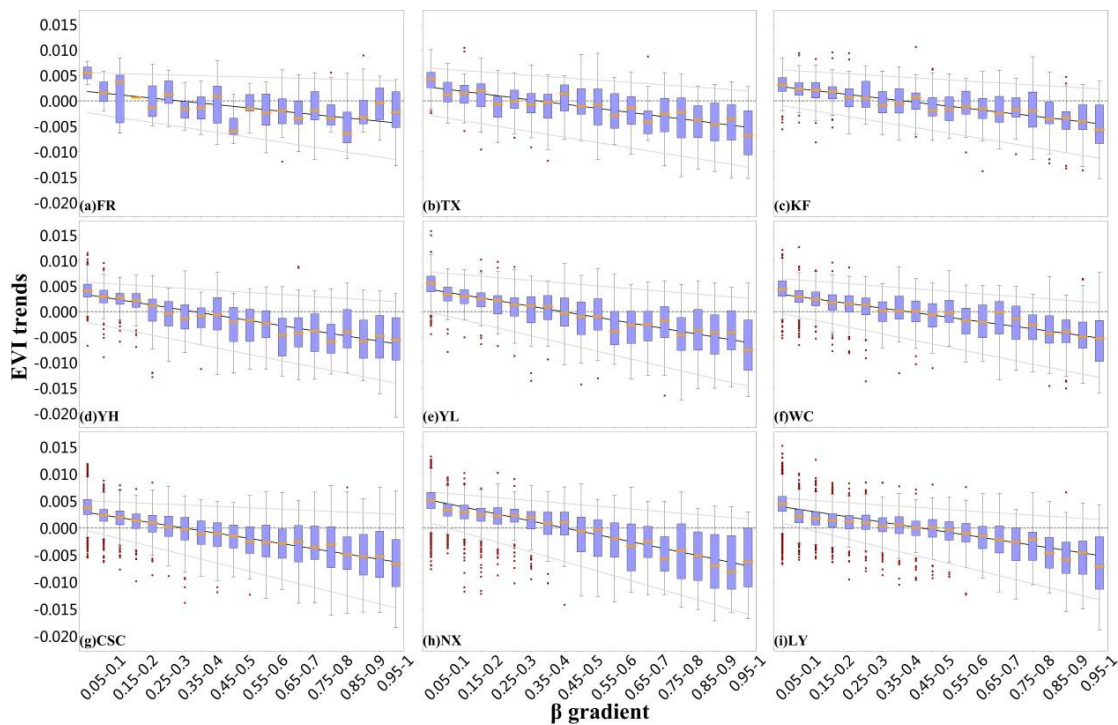
179 We used linear regression analyses to explore the relationships between the indirect  
180 effects, the growth offset, and  $\beta$  of each year at 250-m resolution in Changsha from 2000 to  
181 2017. The growth offset was calculated as the average within each urbanization intensity  
182  $\beta$  bin, defined at 0.01 intervals along the gradient. Then, the inter-annual variation and trends  
183 in the indirect effects during 2000-2017 at 250-m resolution were calculated and analyzed  
184 using Ordinary Least Square regression.

## 185 **3. Results**

### 186 **3.1 EVI trends along urbanization intensity ( $\beta$ ) gradients**

187 The spatial and temporal patterns of EVI trends from 2000 to 2017 showed a large  
188 spatial heterogeneity of vegetation growth response across nine districts of Changsha and  
189 were associated with urbanization intensity (Fig. 1, Fig.S2). The EVI trends ranged from -  
190 0.02 to 0.016, where positive values showed an increase in EVI over the years and negative  
191 values vice versa. Regions with high urbanization levels usually showed a decreasing EVI  
192 trend over the years (Table S1). For example, 64% of areas showed significant decreasing  
193 trends of EVI in the district with the highest average urbanization intensity (i.e., FR), while  
194 only 6.2% of areas had EVI declined over years in the district with the lowest average  
195 urbanization intensity (i.e., LY, Fig. S1, S2). We further quantified the EVI trends from 2000  
196 to 2017 along urbanization intensity based on regional disparity analysis (Fig. 2). EVI trends  
197 showed a decrease from positive to negative values with urbanization intensity, which means,

198 there was a turning point of EVI temporal changes from increasing to decreasing along  $\beta$   
 199 gradient in every district (Fig. 2, Fig. S3). The corresponding  $\beta$  values of the turning point of  
 200 EVI trends varied across regions at different urbanization levels. For example, the turning  
 201 point  $\beta$  values were lower in districts with higher levels of urbanization (i.e., FR, TX, KF, and  
 202 YH, at  $\beta = 0.15-0.25$ ) than in districts with lower levels of urbanization (i.e., YL, WC, CSC,  
 203 NX, and LY, at  $\beta = 0.4-0.5$ ).



204  
 205 **Fig. 2.** Bin-wise (0.05 intervals) boxplots showing changes in vegetation EVI trends from  
 206 2000 to 2017 in nine administrative districts of Changsha along the urbanization intensity ( $\beta$ )  
 207 gradient. The horizontal line in the center of each box is the median, the edges of each box are  
 208 the 25th and 75th percentiles, and the whiskers extend to 1.5 times the interquartile range.  
 209 Red points outside the whiskers are potential outliers. Black lines represent median fitted lines  
 210 and gray lines show the 5% and 95% quantile regression fits. The Gray dotted line shows the  
 211 zero-line of EVI trends.

## 212 **3.2 Vegetation responses to urbanization**

213 **The EVI~ $\beta$  Relationship and its Variability in 2000, 2009, and 2017.** We used the  
214 relationships in 2000, 2009 and 2017, respectively, to initially examine the details of the  
215 temporal variation of the EVI~ $\beta$  relationship (Fig. S4). Overall, the relationships were all  
216 statistically significant with cubic regression fits, and EVI all decreased with urbanization  
217 intensity. However, there were differences in the shape of the relationship over the three years,  
218 showing significant temporal variation. The y-intercept of the EVI~ $\beta$  relationship was higher  
219 in 2017 compared with that in 2000, representing a temporal increase of maximum EVI in  
220 natural areas without urbanization impacts. The positive enhancement by urbanization on EVI  
221 was indicated by the differences between EVI values and the zero-impact line (also called  
222 indirect EVI change) from the shape of the EVI~ $\beta$  relationship. Importantly, about 77%, 81%  
223 and 94% of the urban intensity bins recorded EVI enhancement in 2000, 2009 and 2017  
224 respectively, representing a potential temporal evolution of the impacts of urbanization on  
225 vegetation growth along urban intensity gradient across years.

226 **Temporal Enhancement of EVI~ $\beta$  Relationships.** We extracted EVI-related parameters  
227 from the EVI~ $\beta$  relationships and overlaid the annual relationships between the parameters  
228 and  $\beta$  gradient from 2000 to 2017, whereby the temporal evolution of the impacts of  
229 urbanization on EVI was quantified, resulting in the most important results that can be  
230 presented from three perspectives (Fig. 3).

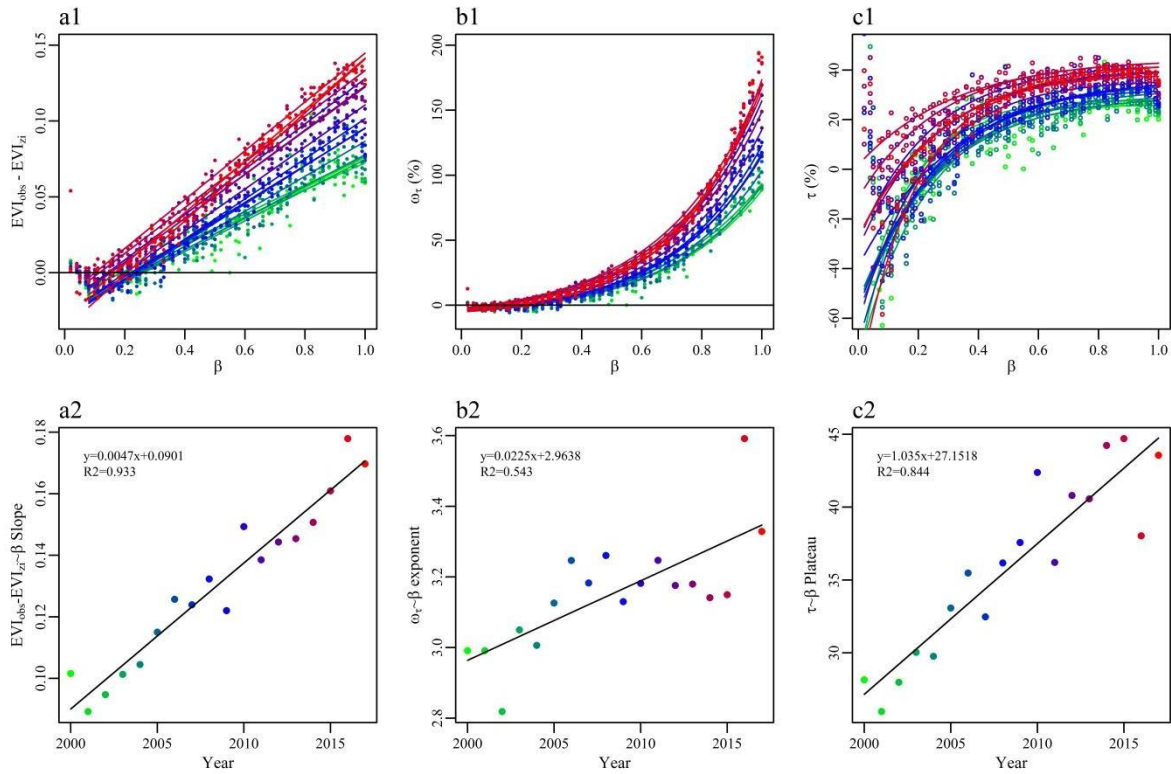
231 First, from the perspective of indirect EVI change~ $\beta$  gradient relationship, indirect EVI  
232 change caused by urbanization showed an increasing trend with  $\beta$  gradient in all years (Fig.  
233 3a1). In addition, the lines of the relationships became steeper over the years, as shown by the  
234 slopes of the relationships exhibiting a linear enhancement with time (Fig. 3a2), and a 1.8-fold

235 increase in slopes from 2000 (0.09) to 2017 (0.17). The results clearly show positive  
236 enhancement of vegetation growth by urbanization was not only increasing with urban  
237 intensity but also intensifying with time.

238 Second, the relative impact of urbanization on EVI ( $\omega$ , quantified by the ratio of indirect  
239 EVI change to EVI without urbanization impacts) showed a superlinearly increase along the  $\beta$   
240 gradient in all years (Fig. 3b1). Similarly, the superlinear growth scaling exponent of the  
241 relationship also showed a linear increase in time, varying from 2.99 in 2000 to 3.33 in 2017  
242 (Fig. 3b2). Such superlinear growth relationships suggested that vegetation in high urban  
243 intensity regions ( $\beta > 0.6$ ) was much more positively sensitive to urbanization than vegetation  
244 in lower urban intensity regions, suggesting temporal indirect enhancement was more  
245 pronounced in high urban intensity areas. For example, the relative impact of urbanization on  
246 vegetation can be doubled from 2000 (90%) to 2017 (180%) in the highest urban intensity  
247 areas ( $\beta$  close to 1).

248 Third, the EVI compensation effect by urbanization positive impact increased sublinearly  
249 along urbanization intensity, showing maximum effects at  $\beta > 0.8$ , implying a potential  
250 compensation threshold in urban environments (Fig. 3c1). The maximum compensation effect  
251 also showed a linear increasing trend with the year (Fig. 3c2), and the vegetation growth  
252 enhancement offset about 28% of the direct surface-replacement impact in 2000 rising to 44%  
253 in 2017.





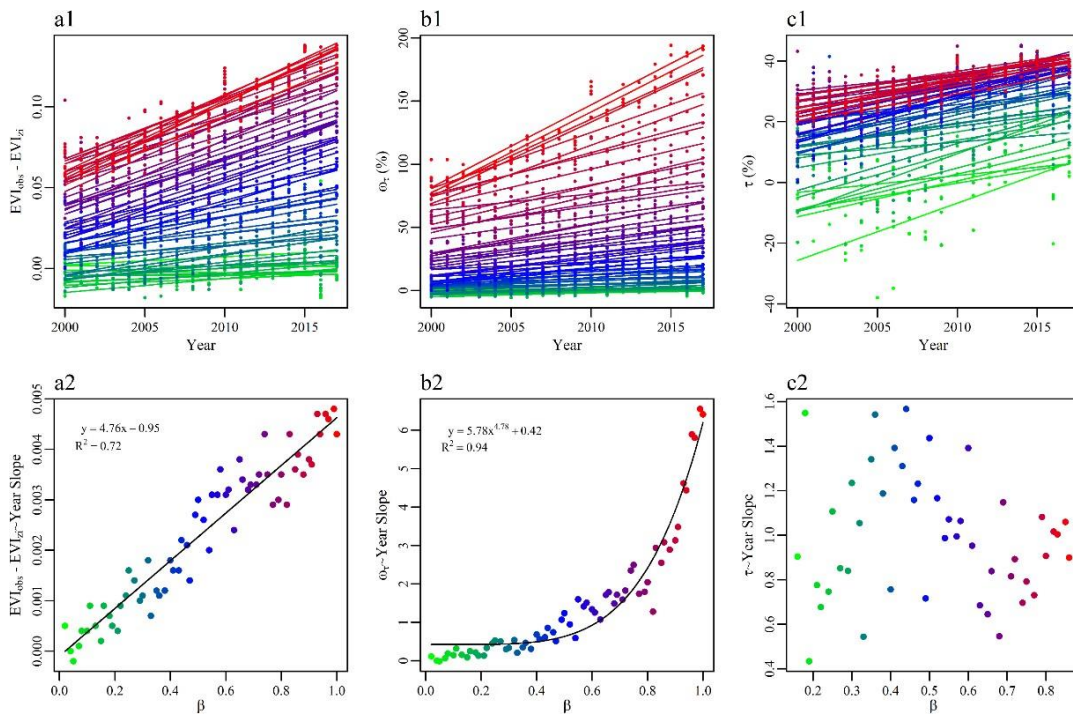
254

255 **Fig. 3.** Temporal dynamics of relationships between EVI-related parameters and urbanization  
 256 intensity ( $\beta$ ) during 2000-2017:  $\beta$ -dependent growth enhancement (i.e., EVI change caused by  
 257 urbanization or indirect effect) (a1); change of the linear dependence of growth enhancement  
 258 on  $\beta$  (i.e., yearly slopes in a1) with time (a2);  $\beta$ -dependent relative growth enhancement ( $\omega$ ) of  
 259 urbanization (b1); regression exponent (in b1) change with time (b2);  $\beta$ -dependent EVI  
 260 compensation ( $\tau$ ) by growth enhancement (c1); and temporal change of the maximum  
 261 compensation effects (asymptotes in c1) (c2). The color gradient (from green to blue to red)  
 262 represents the change in time from 2000 to 2017.

263 **Differences in the  $\beta$  Dependence of EVI~Time Relationships.** We established the  
 264 linear relationships between key EVI-related parameters (i.e., growth enhancement  $EVI_{obs}$ -  
 265  $EVI_{zi}$ , relative growth enhancement  $\omega$ , and offset  $\tau$ ) and time, and found the slopes of the  
 266 relationships increased with urbanization intensity, suggesting the temporal evolution of  
 267 urbanization impacts on vegetation growth (Fig. 4). Both the direct and the relative impact of

268 urbanization on EVI ( $\omega$ ) increased linearly with year in all  $\beta$  gradients (from 0 to 1), and the  
 269 relationships steepened with urbanization intensity, as shown by the slopes increasing with  $\beta$   
 270 (Fig4. a1, a2, b1, b2). Particularly, the superlinear growth relationship of the slopes of the  
 271  $\omega$ -year relationship along the  $\beta$  gradient indicated that the relative growth enhancement of  
 272 vegetation responded superlinearly to urbanization intensity (i.e., the more intense the  
 273 urbanization, the faster the increase of the  $\omega$ -year slope) (Fig. 4b2).

274 Furthermore, the EVI compensation effect also increased linearly with years, however,  
 275 the growth sensitivities (slopes) of such relationships did not show an obvious increasing or  
 276 decreasing trend along the  $\beta$  gradient (Fig. 4c1, 4c2), manifesting a converged similarity  
 277 across all districts (Fig. S5).

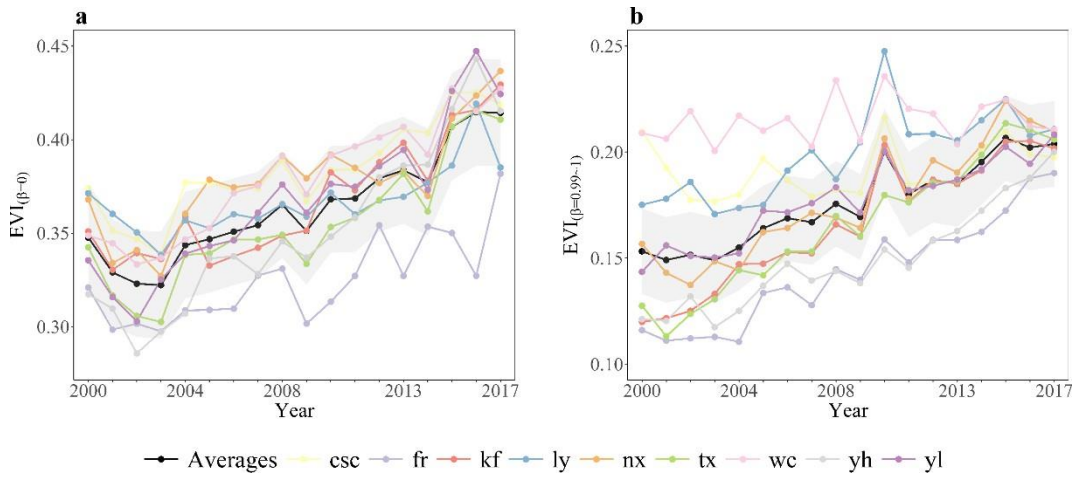


278  
 279 **Fig. 4.** Relationship between EVI-related parameters and time, and their changes along an  
 280 urbanization intensity ( $\beta$ ) gradient. The gradient colors (from green to blue to red) represent  
 281 the change in urbanization intensity (from 0 to 1). Plots in the upper row represent the

282 relationships between times (from 2000 to 2017) and (a1) EVI growth enhancement; (b1) the  
283 relative growth enhancement ( $\omega$ ) of urbanization; and (c1) the EVI compensation by growth  
284 enhancement ( $\tau$ ). Figures in the lower row (a2, b2, c3) represent the evolution of the  
285 regression slopes shown in the upper row (a1, b1, and c1, respectively) along  $\beta$ .

### 286 **3.3 EVI in rural and highly urbanized areas**

287 Further, EVI in rural and highly urbanized areas showed a generally upward trend over  
288 time (Fig. 5). The EVI in rural areas increased from about 0.33 to 0.41 on average during the  
289 study period ( $\beta=0$ , Fig 5a), although the magnitude of increase was district-specific and  
290 dependent on the initial EVI. The increasing trends of EVI in rural areas were similar among  
291 all districts. The annual average EVI in highly urban areas in different districts increased  
292 gradually over time and converged towards 0.22 in all districts (Fig. 5b). The increasing  
293 trends of EVI in highly urban areas were different among all districts, depending on the  
294 urbanization development priority sequence of districts. For instance, districts prioritized for  
295 development first (e.g., FR, KF, TX) had a low initial EVI in 2000 (around 0.13), and EVI  
296 exhibited an obvious upward convergence to 0.22. While districts with no priority for  
297 development (e.g., LY, CSC, WC) had a higher initial EVI (around 0.17-0.22) and showed  
298 interannual fluctuations around  $EVI=0.22$  during 2000-2017.



299  
 300 **Fig. 5.** Comparison of EVI corresponding to (a) fully vegetated ( $\beta = 0$ ) and (b) highly  
 301 urbanized ( $\beta = 0.99 \sim 1$ ) areas from 2000 to 2017 in nine administrative regions. The shaded  
 302 area represents the 95% confidence interval of the average EVI change.

## 303 4. Discussion

### 304 4.1. Regional disparity of temporal evolution in EVI changes

305 Our results provided a new insight into the regional disparity of temporal evolution in  
 306 vegetation growth by urbanization impacts (Fig. 2). A few studies have discovered a prevalent  
 307 enhancement impact of urbanization on vegetation growth (Jia et al., 2018; Zhao et al., 2016;  
 308 Zhou et al., 2014). However, they often focused on vegetation growth change with  
 309 urbanization intensity gradient within cities, or compared vegetation growth between urban  
 310 core and fringe areas (Guan et al., 2019; Gui et al., 2019; Li et al., 2020; Zhong et al., 2019).  
 311 Our study further quantified the response of vegetation not only across urbanization intensity  
 312 but also the spatial heterogeneity among various districts at different urbanization levels,  
 313 depicting a dynamic trend of EVI changes as urbanization proceeds. Thus, our study  
 314 emphasized the importance of considering the levels and process of urbanization more

315 accurately to better manifest the spatial heterogeneity of the co-evolution of vegetation  
316 growth and urbanization-induced environments, therefore shed new light on the dynamic  
317 response of vegetation growth to urbanization at a large scale.

## 318 **4.2. Temporal vegetation growth in rural and highly urbanized** 319 **areas**

320 Although EVI temporal changes include both changes in vegetated cover areas and  
321 vegetation growth (Yuan et al., 2007), our results have described interannual increasing trends  
322 in vegetation growth by focusing on two special  $\beta$  bins (i.e.,  $\beta=0$  completely covered by  
323 vegetation and  $\beta=0.99\sim 1$  highly urbanized areas) to exclude the interference of changing  
324 vegetation areas (Fig. 5). Generally, the temporal increase of vegetation growth in natural  
325 vegetated areas may be attributed to climate change, whereas in highly urbanized areas may  
326 confirm the positive impact of urbanization on vegetation enhancement.

327 In natural vegetated areas, EVI increase in our study area (Fig. 5a) is consistent with a  
328 remote sensing-derived study that reported that China is a vegetation greening hotspot since  
329 2000 (Piao et al., 2019), which might be mainly contributed to CO<sub>2</sub> fertilization and global  
330 warming. Given the location of Changsha is in a warm-humid region with sufficient nutrient  
331 and water availability, the CO<sub>2</sub> fertilization effect plays a full role in enhancing photosynthesis  
332 and water use efficiency leading to vegetation greening (Hickler et al., 2008; Huang et al.,  
333 2017; Schimel et al., 2015; Zhu et al., 2016). The temperature increase may also be the reason  
334 for EVI increase by enhancing metabolism and extending the growing season (Braswell et al.,  
335 1997; Piao et al., 2007; Richardson et al., 2010).

336 There is an emergent trend in vegetation growth toward an asymptotic maximum  
337 response as urbanization proceeds (Fig 5b). In highly urbanized areas, our study reported the

338 annual growth trends of EVI, which further expands the existing understanding of the impact  
339 of urbanization on vegetation greening. There is prevalent vegetation greening over time in  
340 the urban core (Li et al., 2020; Liu and Gong, 2012; Liu et al., 2015b; Zhong et al., 2019;  
341 Zhou et al., 2014), however, most of these results are based on annual maps of greenness  
342 indices changes and do not quantify the spatial-temporal dynamics. Our results not only found  
343 a dynamic increase in vegetation growth over time, but also made a pathbreaking discovery  
344 that there may be an upper limit to this increase (Fig. 5b). The increasing tendency of EVI  
345 could be attributed to the positive effects derived from a changing urban environment, such as  
346 localized warming, CO<sub>2</sub>, and nitrogen enrichment, and the improvement of management and  
347 maintenance of urban green space (Elmore et al., 2012; Gregg et al., 2003; Imhoff et al.,  
348 2004b; Jia et al., 2018; Jia et al., 2021; Pretzsch et al., 2017; Zhao et al., 2016). We further  
349 found the average EVI gradually narrowed and converged to 0.22 (Fig. 5b). This means in  
350 areas with little vegetation (e.g.,  $\beta=0.99-1$ ), the promotion effect of urbanization on vegetation  
351 growth becomes saturated over time because of vegetation adaptation limit. This case  
352 suggests that vegetation growth cannot be simply enhanced through warming urban  
353 environments or management measures but by increasing the vegetation cover. Further, that  
354 indicates a possible pattern of future vegetation growth if we regard the urban environment as  
355 the surrogate of future global change. We speculate that the saturation of urbanization effects  
356 on vegetation growth is pervasive in cities, depending on city-specific maximum EVI value  
357 determined by climate zone, water availability, growing season length, species types, and  
358 composition.

### 359 4.3. Positive effects of urbanization on vegetation growth as a 360 function of $\beta$ and time

361 The most important finding of this study was the relationship between the positive effects  
362 of urbanization and  $\beta$  was not stable across years, but rather demonstrated a clear pattern of  
363 temporal evolution showing a 1.8-fold increase in vegetation growth from 2000 to 2017 (Fig.  
364 3 and Fig. 4). The time-variant  $EVI_{en} \sim \beta$  relationship is different from the findings of Zhao et  
365 al. (2016) and Jia et al. (2018), who compared the city-specific regression coefficients  
366 between EVI and urbanization intensity in three time periods (2000, 2006 and 2011), and  
367 found that the  $EVI_{en} \sim \beta$  relationship had strong temporal stability (Jia et al., 2018; Zhao et al.,  
368 2016). However, the regression coefficient variation they compared may be instantaneous and  
369 pulsatile over limited periods, and might not be able to capture the gradual temporal responses  
370 of vegetation. We quantified the models to elucidate the relationship between urbanization's  
371 positive impacts ( $EVI_{en}$ ),  $\beta$ , and time as follows.

372 The dependence of  $EVI_{en}$  on  $\beta$  and time can be further revealed by examining the  
373 relationship between  $EVI_{en}$  and time fitted by  $\beta$  bin (Fig. 3a1, a2).  $EVI_{en}$  increased with time (t  
374 in the year) linearly for all  $\beta$  bins:

$$375 \quad EVI_{en} = k \times (t - 2000) + c \quad (5)$$

376 and the slope (k) increased with  $\beta$ :

$$377 \quad k = b \times \beta + a \quad (6)$$

378 and the intercept (c) increased with  $\beta$ :

$$379 \quad c = d \times \beta + f \quad (7)$$

380 Combining equations (5), (6) and (7), the  $EVI_{en}$  can be calculated as follows:

381 
$$\frac{EVI_{en}}{+f} = b \times \beta \times (t - 2000) + a \times (t - 2000) + d \times \beta \quad (8)$$

382 For Changsha, the coefficients were:  $b=4.76$ ,  $a=-0.95$ ,  $d=0.08$ , and  $f=-0.02$ .

383 Following the same logic for deriving  $EVI_{en}$ ,  $\omega$  can be calculated as follows:

384 
$$\omega = \frac{m \times \beta^g(t - 2000) + n \times (t - 2000) + p \times \beta + q}{\beta + q} \quad (9)$$

385 For Changsha, the coefficients were:  $m=5.78$ ,  $g=4.78$ ,  $n=0.42$ ,  $p=85.5$ , and  $q=-22.2$ . For  
386 convenience, time  $t$  in some expressions above was subtracted by 2000, the starting year of  
387 our analysis.

388 Our models are the first to successfully quantify and predict vegetation growth and the  
389 long-term impact of urbanization on vegetation. One difference that highlights our study from  
390 others is that we quantify the impacts of urbanization-induced environments on vegetation  
391 growth by exhibiting an interannual EVI enhancement in the same  $\beta$  bins (Fig. 3), which  
392 excluded the vegetated area increase through urban maintenance measures. Temporal increase  
393 of the impacts of urbanization on vegetation growth is mainly attributed to the temporal  
394 intensification of urban environments as urbanization continuously proceeds, and implies the  
395 continuous physiological adaptation process of vegetation to urban environments. Based on  
396 this, it is understandable why the EVI evolves more strongly over time in regions with high  
397 urbanization intensity ( $\beta > 0.6$ , Fig. 4b1, 4b2). Urban environment incorporates a myriad of  
398 driving forces to plant growth, such as localized warming,  $CO_2$  and nitrogen enrichment,  
399 ozone, air pollutants, and traffic volume (Imhoff et al., 2004a; Ning et al., 2022; Ning et al.,  
400 2023; Pei et al., 2013; Shu et al., 2022; Takagi and Gyokusen, 2004), which all evolve over  
401 time (Liu et al., 2017). Many studies have ever focused on non-urban ecosystems and  
402 emphasized the importance of time in considering ecosystem response to intensified climate  
403 changes (Dieleman et al., 2012; Luo et al., 2004; Norby et al., 2010; Norby and Zak, 2011;



404 Reich et al., 2006). Our results demonstrated a continuous adaptation and growth  
405 enhancement of vegetation over time in urban ecosystems. Urbanization-induced  
406 environments are considered the harbinger of future global change in other ecosystems  
407 (Grimm et al., 2008). Our study confirmed a possibility of future vegetation growth response  
408 based on the temporal evolution, in addition, our proposed model also demonstrated that  
409 future urban vegetation growth could be predicted by the urban intensity and time. Moreover,  
410 although we cannot directly translate the EVI enhancement into net carbon gain, owing to the  
411 offsetting effect of increased soil carbon decomposition (Zhao et al., 2016), our findings still  
412 highlight the importance of considering vegetation in urbanized areas within the terrestrial  
413 carbon cycle and predicting plant adaptation under future conditions as cities continue to  
414 evolve over time and across the globe.

#### 415 **4.4. The offsetting effect became stronger over time**

416 Our results demonstrated that vegetation growth compensation capacity from  
417 urbanization, positive effect minus vegetation loss by urban expansion, reached a peak in  
418 regions with high urbanization intensity (e.g.,  $\beta > 0.8$ ), which strengthened over the years  
419 (from 28% in 2000 to 44% in 2017, Fig. 3, 4). The patterns of the offset effect with  
420 urbanization intensity gradient may be related to regional heterogeneity of urban  
421 development, background vegetation cover, and city location (Jia et al., 2018; Zhong et al.,  
422 2019). For example, the offset effect was generally lower in regions with higher background  
423 vegetation cover, lower urbanization levels and better vegetation growth conditions (Jia et al.,  
424 2018). It was reported the mode of offset percentage was almost invariant across urbanization  
425 intensity gradient in multiple cities (Jia et al., 2018; Zhao et al., 2016), which provides a  
426 general pattern but ignored the heterogeneity of individual cities. We emphasized the  
427 maximum growth enhancement offset effects become stronger over time, which should be

428 related to the continuous temporal increase of positive enhancement by urbanization shown in  
429 this study. Urban areas have been expanding over the years, resulting in continuous loss of  
430 vegetation due to land conversion, while our research shows that temporal environmental  
431 changes caused by urbanization can promote the enhancement of residual vegetation growth  
432 to compensate for vegetation loss caused by urbanization. Further quantification of long-term  
433 annual changes in the urbanization intensity-offset effect relationship can support a deeper  
434 understanding of urban ecology, which is of great significance for realizing the sustainable  
435 development goals of human society in an increasingly urbanized world.

## 436 **5. Conclusion**

437 Our study quantified the temporal evolution of urbanization impacts on vegetation growth  
438 by using annual time-series remote sensing images by expanding Zhao and colleagues'  
439 framework. Overall, the EVI temporal trends showed a general increasing trend in less  
440 urbanized areas and a decreasing trend in highly urbanized areas in all districts. More  
441 importantly, our study revealed the intensification of the vegetation growth enhancement over  
442 time across all districts in Changsha. Specifically, we found the indirect growth enhancement  
443 effects increased with urbanization intensity and the power of the effects (slope and exponent  
444 of the relationships) increased with time as well; moreover, the maximum offsetting effects  
445 from growth enhancement effects became stronger over time (from 28% in 2000 to 44% in  
446 2017). We further developed a model to predict the positive effect of urbanization on  
447 vegetation growth by using urbanization intensity and time, which can be verified in more  
448 cities in the future.

449 Our study is a successful first attempt to explore the long-term spatial-temporal pattern of  
450 urbanization and vegetation co-evolution. Future research is expected to extend our

451 framework to more cities and stress the importance of time. One implication of our results is  
452 that EVI enhancement in urban environments over time could be an indicator of increasing  
453 productivity globally, leading to changes of carbon sources and sinks at different spatial and  
454 temporal scales owing to continuous urban expansion. Understanding the response of  
455 vegetation to urbanization based on long-term observations could provide new insight into  
456 interactions and co-evolution of multiple global-change drivers and adaptation strategies of  
457 plants.

458

## 459 **Acknowledgments**

460 This work was supported by research grants from the National Natural Science  
461 Foundation of China (U20A2089 and 41971152) and Natural Science Foundation of Jiangsu  
462 Province of China (BK20220019) to SL, and the Hunan Provincial Innovation Foundation For  
463 Postgraduate (CX20200703), and Scientific Innovation Fund for Post-graduates of Central  
464 South University of Forestry and Technology (CX20201011) to XP. We thank Qi Zhang,  
465 Yuanyuan Li, and Rui Guo for their comments on the draft.

## 466 **Declaration of Interest Statement:**

467 All authors disclose any actual or potential conflict of interest including any financial,  
468 personal, or other relationships with other people or organizations within three years of  
469 beginning the work submitted that might inappropriately influence, or be perceived as  
470 influencing, their work.

## 471 **Data availability statement**

472 All original datasets used in this study are available from the respective references, with  
473 most being open access. The generated data that form the results of this study are available  
474 from the corresponding author upon reasonable request.

## 475 **Author Contributions**

476 Xi Peng: Formal analysis, Writing – original draft; Shucheng Jiang: Data curation,  
477 Writing – original draft; Shuguang Liu: Conceptualization, Methodology, Supervision,  
478 Writing – original draft, Writing – review & editing, Funding acquisition; Yang Zhan, Yi Shi:  
479 Formal analysis, Writing – review & editing; Rubén Valbuena, Andy Smith: Validation,  
480 Writing – review & editing; Ying Ning, Shuailong Feng, Haiqiang Gao and Zhao Wang:  
481 Writing – review & editing.

## 482 **References**

483 Braswell, B., Schimel, D.S., Linder, E. and Moore, B. 1997. The response of global  
484 terrestrial ecosystems to interannual temperature variability. *Science* 278(5339), 870-  
485 873.

486 Chen, B., Xu, B., Zhu, Z., Yuan, C., Suen, H.P., Guo, J., Xu, N., Li, W., Zhao, Y., and Yang, J.  
487 2019. Stable classification with limited sample: Transferring a 30-m resolution  
488 sample set collected in 2015 to mapping 10-m resolution global land cover in 2017.  
489 *Science Bulletin* 64, 370-373.

490 de Jong, M., Yu, C., Joss, S., Wennersten, R., Yu, L., Zhang, X. and Ma, X. 2016. Eco city

491 development in China: addressing the policy implementation challenge. *Journal of*  
492 *Cleaner Production* 134, 31-41.

493 Dieleman, W.I., Vicca, S., Dijkstra, F.A., Hagedorn, F., Hovenden, M.J., Larsen, K.S.,  
494 Morgan, J.A., Volder, A., Beier, C. and Dukes, J.S. 2012. Simple additive effects are  
495 rare: a quantitative review of plant biomass and soil process responses to combined  
496 manipulations of CO<sub>2</sub> and temperature. *Global change biology* 18(9), 2681-2693.

497 Elmore, A.J., Guinn, S.M., Minsley, B.J. and Richardson, A.D. 2012. Landscape controls  
498 on the timing of spring, autumn, and growing season length in mid- Atlantic forests.  
499 *Global Change Biology* 18(2), 656-674.

500 Fang, J. 2004. Increasing terrestrial vegetation activity in China, 1982-1999. *Science in*  
501 *China Series C* 47(3).

502 Gong, P., Li, X. and Zhang, W. 2019. 40-Year (1978-2017) human settlement changes in  
503 China reflected by impervious surfaces from satellite remote sensing. *Science Bulletin*  
504 64(11), 756-763.

505 Gregg, J.W., Jones, C.G. and Dawson, T.E. 2003. Urbanization effects on tree growth in the  
506 vicinity of New York City. *Nature* 424(6945), 183-187.

507 Grimm, N.B., Faeth, S.H., Golubiewski, N.E., Redman, C.L., Wu, J., Bai, X. and Briggs, J.M.  
508 2008. Global change and the ecology of cities. *science* 319(5864), 756-760.

509 Guan, X., Shen, H., Li, X., Gan, W. and Zhang, L. 2019. A long-term and comprehensive  
510 assessment of the urbanization-induced impacts on vegetation net primary  
511 productivity. *Sci Total Environ* 669, 342-352.

512 Gui, X., Wang, L., Yao, R., Yu, D. and Li, C. 2019. Investigating the urbanization process

513 and its impact on vegetation change and urban heat island in Wuhan, China.  
514 Environmental Science and Pollution Research 26(30), 30808-30825.

515 He, B., Chen, A., Wang, H. and Wang, Q. 2015. Dynamic response of satellite-derived  
516 vegetation growth to climate change in the Three North Shelter Forest Region in  
517 China. Remote Sensing 7(8), 9998-10016.

518 Hickler, T., Smith, B., Prentice, I.C., Mjöfors, K., Miller, P., Arneth, A. and Sykes, M.T.  
519 2008. CO2 fertilization in temperate FACE experiments not representative of boreal  
520 and tropical forests. Global Change Biology 14(7), 1531-1542.

521 Huang, M., Piao, S., Janssens, I.A., Zhu, Z., Wang, T., Wu, D., Ciais, P., Myneni, R.B.,  
522 Peaucelle, M. and Peng, S. 2017. Velocity of change in vegetation productivity over  
523 northern high latitudes. Nature ecology & evolution 1(11), 1649-1654.

524 Hutyra, L.R., Yoon, B. and Alberti, M. 2011. Terrestrial carbon stocks across a gradient of  
525 urbanization: a study of the Seattle, WA region. Global Change Biology 17(2), 783-  
526 797.

527 Imhoff, M.L., Bounoua, L., DeFries, R., Lawrence, W.T., Stutzer, D., Tucker, C.J. and  
528 Ricketts, T. 2004a. The consequences of urban land transformation on net primary  
529 productivity in the United States. Remote Sensing of Environment 89(4), 434-443.

530 Imhoff, M.L., Bounoua, L., Ricketts, T., Loucks, C., Harriss, R. and Lawrence, W.T. 2004b.  
531 Global patterns in human consumption of net primary production. Nature 429(6994),  
532 870-873.

533 Jia, W., Zhao, S. and Liu, S. 2018. Vegetation growth enhancement in urban environments  
534 of the Conterminous United States. Glob Chang Biol 24(9), 4084-4094.

535 Jia, W., Zhao, S., Zhang, X., Liu, S., Henebry, G.M. and Liu, L. 2021. Urbanization imprint  
536 on land surface phenology: The urban–rural gradient analysis for Chinese cities.  
537 *Global Change Biology* 27(12), 2895-2904.

538 Li, D., Wu, S., Liang, Z. and Li, S. 2020. The impacts of urbanization and climate change  
539 on urban vegetation dynamics in China. *Urban Forestry & Urban Greening* 54.

540 Li, J., Li, C., Zhu, F., Song, C. and Wu, J. 2013. Spatiotemporal pattern of urbanization in  
541 Shanghai, China between 1989 and 2005. *Landscape ecology* 28(8), 1545-1565.

542 Liu, M., Liu, S., Ning, Y., Zhu, Y., Valbuena, R., Guo, R., Li, Y., Tang, W., Mo, D. and Rosa,  
543 I. 2020. Co-Evolution of Emerging Multi-Cities: Rates, Patterns and Driving  
544 Policies Revealed by Continuous Change Detection and Classification of Landsat  
545 Data. *Remote Sensing* 12(18), 2905.

546 Liu, S., Bond-Lamberty, B., Boysen, L.R., Ford, J.D., Fox, A., Gallo, K., Hatfield, J.,  
547 Henebry, G.M., Huntington, T.G., Liu, Z., Loveland, T.R., Norby, R.J., Sohl, T.,  
548 Steiner, A.L., Yuan, W., Zhang, Z. and Zhao, S. 2017. Grand Challenges in  
549 Understanding the Interplay of Climate and Land Changes. *Earth Interactions* 21(2), 1-  
550 43.

551 Liu, S. and Gong, P. 2012. Change of surface cover greenness in China between 2000 and  
552 2010. *Chinese Science Bulletin* 57(22), 2835-2845.

553 Liu, Y., Li, Y., Li, S. and Motesharrei, S. 2015a. Spatial and Temporal Patterns of Global  
554 NDVI Trends: Correlations with Climate and Human Factors. *Remote Sensing* 7(10),  
555 13233-13250.

556 Liu, Y., Wang, Y., Peng, J., Du, Y., Liu, X., Li, S. and Zhang, D. 2015b. Correlations  
557 between Urbanization and Vegetation Degradation across the World's Metropolises

558 Using DMSP/OLS Nighttime Light Data. *Remote Sensing* 7(2), 2067-2088.

559 Luo, Y., Su, B., Currie, W.S., Dukes, J.S., Finzi, A., Hartwig, U., Hungate, B., McMurtrie,  
560 R.E., Oren, R. and Parton, W.J. 2004. Progressive nitrogen limitation of ecosystem  
561 responses to rising atmospheric carbon dioxide. *Bioscience* 54(8), 731-739.

562 Ning, Y., Liu, S., Smith, A.R., Qiu, Y., Gao, H., Lu, Y., Yuan, W. and Feng, S. 2023.  
563 Dynamic multi-dimensional scaling of 30+ year evolution of Chinese urban systems:  
564 Patterns and performance. *Science of The Total Environment* 863, 160705.

565 Ning, Y., Liu, S., Zhao, S., Liu, M., Gao, H. and Gong, P. 2022. Urban growth rates,  
566 trajectories, and multi-dimensional disparities in China. *Cities* 126, 103717.

567 Norby, R.J., Warren, J.M., Iversen, C.M., Medlyn, B.E. and McMurtrie, R.E. 2010. CO<sub>2</sub>  
568 enhancement of forest productivity constrained by limited nitrogen availability. *Proc*  
569 *Natl Acad Sci U S A* 107(45), 19368-19373.

570 Norby, R.J. and Zak, D.R. 2011. Ecological Lessons from Free-Air CO<sub>2</sub> Enrichment  
571 (FACE) Experiments. *Annual Review of Ecology, Evolution, and Systematics* 42(1),  
572 181-203.

573 Pei, F., Li, X., Liu, X., Wang, S. and He, Z. 2013. Assessing the differences in net primary  
574 productivity between pre-and post-urban land development in China. *Agricultural and*  
575 *forest meteorology* 171, 174-186.

576 Piao, S., Friedlingstein, P., Ciais, P., Viovy, N. and Demarty, J. 2007. Growing season  
577 extension and its impact on terrestrial carbon cycle in the Northern Hemisphere over  
578 the past 2 decades. *Global Biogeochemical Cycles* 21(3).

579 Piao, S., Wang, X., Park, T., Chen, C., Lian, X., He, Y., Bjerke, J.W., Chen, A., Ciais, P.,



580 Tømmervik, H., Nemani, R.R. and Myneni, R.B. 2019. Characteristics, drivers and  
581 feedbacks of global greening. *Nature Reviews Earth & Environment* 1(1), 14-27.

582 Pretzsch, H., Biber, P., Uhl, E., Dahlhausen, J., Schutze, G., Perkins, D., Rotzer, T., Caldentey,  
583 J., Koike, T., Con, T.V., Chavanne, A., Toit, B.D., Foster, K. and Lefer, B. 2017.  
584 Climate change accelerates growth of urban trees in metropolises worldwide. *Sci Rep*  
585 7(1), 15403.

586 Reich, P.B., Hungate, B.A. and Luo, Y. 2006. Carbon-nitrogen interactions in terrestrial  
587 ecosystems in response to rising atmospheric carbon dioxide. *Annu. Rev. Ecol. Evol.*  
588 *Syst.* 37, 611-636.

589 Richardson, A.D., Andy Black, T., Ciais, P., Delbart, N., Friedl, M.A., Gobron, N., Hollinger,  
590 D.Y., Kutsch, W.L., Longdoz, B. and Luysaert, S. 2010. Influence of spring and  
591 autumn phenological transitions on forest ecosystem productivity. *Philosophical*  
592 *Transactions of the Royal Society B: Biological Sciences* 365(1555), 3227-3246.

593 Schimel, D., Stephens, B.B. and Fisher, J.B. 2015. Effect of increasing CO<sub>2</sub> on the  
594 terrestrial carbon cycle. *Proceedings of the National Academy of Sciences* 112(2),  
595 436-441.

596 Sen, P.K. 1968. Estimates of the regression coefficient based on Kendall's tau. *Journal of*  
597 *the American statistical association* 63(324), 1379-1389.

598 Shi, Y., Liu, S., Yan, W., Zhao, S., Ning, Y., Peng, X., Chen, W., Chen, L., Hu, X. and Fu, B.  
599 2021. Influence of landscape features on urban land surface temperature: Scale and  
600 neighborhood effects. *Science of the Total Environment* 771, 145381.

601 Shu, Y., Liu, S., Wang, Z., Xiao, J., Shi, Y., Peng, X., Gao, H., Wang, Y., Yuan, W. and Yan, W.  
602 2022. Effects of Aerosols on Gross Primary Production from Ecosystems to the

603 Globe. Remote Sensing 14(12), 2759.

604 Takagi, M. and Gyokusen, K. 2004. Light and atmospheric pollution affect photosynthesis  
605 of street trees in urban environments. Urban forestry & urban greening 2(3), 167-171.

606 Tang, W., Liu, S., Kang, P., Peng, X., Li, Y., Guo, R., Jia, J., Liu, M. and Zhu, L. 2021.  
607 Quantifying the lagged effects of climate factors on vegetation growth in 32 major  
608 cities of China. Ecological Indicators 132, 108290.

609 Youngsteadt, E., Dale, A.G., Terando, A.J., Dunn, R.R. and Frank, S.D. 2015. Do cities  
610 simulate climate change? A comparison of herbivore response to urban and global  
611 warming. Glob Chang Biol 21(1), 97-105.

612 Yu, M., Gao, Q., Gao, C. and Wang, C. 2017. Extent of night warming and spatially  
613 heterogeneous cloudiness differentiate temporal trend of greenness in mountainous  
614 tropics in the new century. Scientific reports 7(1), 1-10.

615 Yuan, W., Liu, S., Zhou, G., Zhou, G., Tieszen, L.L., Baldocchi, D., Bernhofer, C., Gholz, H.,  
616 Goldstein, A.H. and Goulden, M.L. 2007. Deriving a light use efficiency model  
617 from eddy covariance flux data for predicting daily gross primary production across  
618 biomes. Agricultural and Forest Meteorology 143(3-4), 189-207.

619 Zhang, L., Yang, L., Zohner, C.M., Crowther, T.W., Li, M., Shen, F., Guo, M., Qin, J., Yao, L.,  
620 and Zhou, C. 2022. Direct and indirect impacts of urbanization on vegetation  
621 growth across the world's cities. Science Advances 8(27), eabo0095.

622 Zhang, S., Jia, W., Zhu, H., You, Y., Zhao, C., Gu, X. and Liu, M. 2023. Vegetation growth  
623 enhancement modulated by urban development status. Science of The Total  
624 Environment, 163626.

- 625 Zhao, A., Zhang, A., Cao, S., Liu, X., Liu, J. and Cheng, D. 2018. Responses of vegetation  
626 productivity to multi-scale drought in Loess Plateau, China. *Catena* 163, 165-171.
- 627 Zhao, S., Liu, S. and Zhou, D. 2016. Prevalent vegetation growth enhancement in urban  
628 environment. *Proc Natl Acad Sci U S A* 113(22), 6313-6318.
- 629 Zhong, Q., Ma, J., Zhao, B., Wang, X., Zong, J. and Xiao, X. 2019. Assessing spatial-  
630 temporal dynamics of urban expansion, vegetation greenness and photosynthesis in  
631 megacity Shanghai, China during 2000–2016. *Remote Sensing of Environment* 233.
- 632 Zhou, D., Zhao, S., Liu, S. and Zhang, L. 2014. Spatiotemporal trends of terrestrial  
633 vegetation activity along the urban development intensity gradient in China's 32 major  
634 cities. *Sci Total Environ* 488-489, 136-145.
- 635 Zhu, Z., Piao, S., Myneni, R.B., Huang, M., Zeng, Z., Canadell, J.G., Ciais, P., Sitch, S.,  
636 Friedlingstein, P. and Arneeth, A. 2016. Greening of the Earth and its drivers. *Nature*  
637 *climate change* 6(8), 791-795.